Proceedings of the Combustion Institute, Volume 28, 2000/pp. 1693–1699

A NUMERICAL STUDY OF COOL FLAME DEVELOPMENT UNDER MICROGRAVITY

R. FAIRLIE,[1] J. F. GRIFFITHS[2] AND H. PEARLMAN[3]
[1]*Department of Computer Studies*
[2]*School of Chemistry*
The University
Leeds LS2 9JT, UK
[3]*University of Southern California*
Department of Mechanical Engineering
Los Angeles, CA 90089, USA

The existence and spatial development of hydrocarbon cool flames in a spherical vessel under the influence of mass and thermal diffusion have been investigated by numerical methods. The purpose is to examine the nature of the interaction of the physics and chemistry that may drive an oscillatory reaction. The conditions correspond to those that would be experienced at zero gravity, as has been recently put to experimental test. Comparisons and contrasts with responses under perfectly mixed conditions are made. The numerical simulation was based on a skeleton thermokinetic scheme, derived from that of Yang and Gray, in a three-variable model representing two intermediate species and reactant temperature. Dirichlet and Neumann boundary conditions could be variously selected. The equations were cast in one dimension (spherical symmetry) and integrated using the numerical algorithm group routine D03PSF. The reactor surface was assumed to be inert.

Both sustained oscillatory (i.e., multiple) and damped cool flames were predicted to exist under spatially uniform conditions resembling those reported in previous experimental studies. The phase relationship between the chemical species and temperature in sustained oscillation is demonstrated. There was strong evidence for the negative temperature-dependent features. No sustained oscillations were predicted to occur under the effect of diffusive fluxes, although highly damped oscillations were still able to exist. This is compatible with the initial experimental observations in microgravity conditions. The spatial development reveals the growth and decay of the reactive intermediate concentrations, with a corresponding expansion of a combustion front from the center of the reaction system to the edge. High concentrations of intermediates were sustained in the cooler periphery where reaction continued to be supported. Only at abnormally high mass diffusive fluxes could sustained oscillatory reaction be recovered. The dependence of oscillations on the magnitude of mass and thermal diffusion coefficients is explored.

Introduction

Oscillatory (or multiple) cool flames of hydrocarbons and other organic materials in oxygen can be generated in closed or flowing systems at subatmospheric pressures, generally at vessel temperatures in the range 500–700 K, according to the reactant. The accompanying temperature changes may be as much as 200 K. The lowest possible reactant pressures for their occurrence are not less than about 20 kPa (~1/5 atm). This means that under terrestrial conditions, self-heating generates an accompanying natural convection as a result of gravitational effects. Some years ago, Griffiths et al. [1] showed that the buoyancy produced complications in the qualitative structure of the observations and rendered quantitative, theoretical interpretation of the nonlinear, thermokinetic interactions extremely difficult, if not impossible. They also advocated the use of, and developed with others, well-stirred systems both in closed and flowing form [1,2]. Such systems have proved their worth to the fundamental understanding of the oscillatory phenomena, especially because numerical modeling—at the interface between theory and experiment—is most readily applied under spatially uniform conditions. Indeed, the spatially uniform criterion is a prerequisite for the simulation of the non-isothermal oxidation of organic compounds when detailed kinetic models involving enormous numbers of species are exploited [3].

The heat transport process under spatially uniform conditions involves transfer at the interface between the gaseous reactants and the vessel surface and is characterized theoretically and numerically by a

Report Documentation Page

Form Approved
OMB No. 0704-0188

1. REPORT DATE	2. REPORT TYPE	3. DATES COVERED
04 AUG 2000	**N/A**	**-**

4. TITLE AND SUBTITLE	5a. CONTRACT NUMBER
A Numerical Study of Cool Flame Development Under Microgravity	5b. GRANT NUMBER
	5c. PROGRAM ELEMENT NUMBER
6. AUTHOR(S)	5d. PROJECT NUMBER
	5e. TASK NUMBER
	5f. WORK UNIT NUMBER
7. PERFORMING ORGANIZATION NAME(S) AND ADDRESS(ES) **Department of Computer Studies School of Chemistry The University Leeds LS2 9JT, UK**	8. PERFORMING ORGANIZATION REPORT NUMBER
9. SPONSORING/MONITORING AGENCY NAME(S) AND ADDRESS(ES)	10. SPONSOR/MONITOR'S ACRONYM(S)
	11. SPONSOR/MONITOR'S REPORT NUMBER(S)

12. DISTRIBUTION/AVAILABILITY STATEMENT
Approved for public release, distribution unlimited

13. SUPPLEMENTARY NOTES
See also ADM001790, Proceedings of the Combustion Institute, Volume 28. Held in Edinburgh, Scotland on 30 July-4 August 2000.

14. ABSTRACT

15. SUBJECT TERMS

16. SECURITY CLASSIFICATION OF:			17. LIMITATION OF ABSTRACT	18. NUMBER OF PAGES	19a. NAME OF RESPONSIBLE PERSON
a. REPORT	b. ABSTRACT	c. THIS PAGE			
unclassified	**unclassified**	**unclassified**	**UU**	**7**	

(Newtonian) heat transfer coefficient. The simplest foundations for thermal ignition theory were originally derived by Semenov [4] on this same basis. The alternative criterion for heat transport in thermal ignition systems, that of pure conductive heat loss, was developed quantitatively by Frank-Kamenetskii [5], and this foundation was eventually put to quantitative experimental test by Ashmore et al. [6] and Fine et al. [7]. Such tests are possible in gaseous systems because thermal ignition of vapors can be brought about at exceedingly low reactant densities, at which the Rayleigh number is sufficiently low for natural convection to be suppressed.

There is no corresponding opportunity to study oscillatory cool flame phenomena with purely conductive heat loss under terrestrial conditions and so, perhaps, there has been little impetus to investigate their existence and associated spatial structure either theoretically or by numerical analysis, when only diffusive fluxes occur. This contrasts with the lively research activity that prevails with regard to spatial structures of nonlinear, isothermal, kinetic systems [8]. However, an impetus has emerged recently from experimental studies of butane + oxygen cool flames under microgravity conditions by Pearlman and co-workers [9]. The initial studies, on butane + oxygen mixtures in a closed vessel, include an image-intensified photographic record of the cool flame development. Although not unexpected, a striking feature is the perfectly symmetrical development of the chemiluminescence (CH_2O^*) from the center of the reaction vessel, as an expanding circle in the two-dimensional field of view. CH_2O^* is formed only in bimolecular radical interactions, so its intensity is an indicator of where high radical concentrations exist. This development of luminescence contrasts with the buoyancy-driven planar front reported by Griffiths et al. [1] and detected also by Pearlman et al. [9] in their own terrestrial studies which complemented the near zero-gravity experiments. Pearlman and co-workers also found in the initial study that whereas multiple (or oscillatory) cool flames propagated under terrestrial conditions, only one cool flame occurred when heat loss was dominated by thermal diffusion.

These novel experiments inspired us to explore, by numerical analysis, the nature of the interactions involved in thermokinetic oscillations when the chemistry is coupled both to heat and mass transport by diffusive fluxes. To focus on the physical interactions, in particular to examine the way in which diffusive fluxes may control oscillatory events, we have limited the chemistry to a skeleton kinetic scheme. The primary interest under non-isothermal, but non-adiabatic, conditions resides in how a negative temperature coefficient of reaction rate controls the existence of oscillatory reaction, and the way in which the oscillatory behavior may be affected by the mode and magnitude of the heat and mass transport processes involved. To this end, in the present paper we address:

1. The behavior of a simple, kinetic model for spatially uniform, non-isothermal conditions.
2. How, using a one-dimensional, numerical code, the same model behaves when it is exposed to mass and thermal diffusion in spherical symmetry.
3. The spatial structure that develops under the conditions of item no. 2 at Lewis number (Le) = 1, and also when Le is varied.

Kinetic Foundation

The skeleton thermokinetic scheme is derived from the Yang and Gray model [10], but incorporating two intermediate species, which in the context of alkane oxidation may be likened to a free radical propagator (A) and a peroxydic, molecular branching intermediate (B). There are competitive branching and termination reactions with different activation energies. All of the heat is regarded to be generated at the branching cycle. No supplementary propagation processes are considered, which might be the main source of heat release in reality. P is a reactant (or precursor), and C represents final products. One distinction of the role of the precursor from that of a hydrocarbon fuel is that P is deemed not to be involved in any subsequent steps [10,11]. This means that the initiation step can be slowed sufficiently that the computed, time-evolved states approximate well to stationary states of the system because there is no significant perturbation by marked reactant consumption. Damped oscillatory modes are readily distinguished from sustained oscillatory states, in consequence. No activation energy need be assigned to the initiation step when this approach is invoked. The negative temperature dependence of reaction rate (ntc), which is required in a simulation of alkane oxidation, is conferred by the competition of a termination reaction which has a higher activation energy than the branching reaction ($E_{t1} > E_b$). An aged silica vessel, as used in the microgravity study, is expected to be relatively inert to surface termination of intermediates. A weak termination of species B was included to represent this state, the magnitude of which (A_{t2}) determines the lower temperature bound for oscillations. Arrhenius parameters were chosen for the data set to tune the reactive region to be comparable with that of experimental observations, and the exothermicity was chosen to signify the modest heat output associated with low temperature oxidation chemistry. The kinetic scheme and its parameters are shown in Table 1.

This scheme has attributes of the isothermal cubic autocatalytic model developed by Gray and Scott [11], the autocatalytic step of which is replaced by a highly nonlinear, non-isothermal branching step. An

TABLE 1
Kinetic scheme and parameters

		Pre-exponential Factor (s^{-1})	Activation Energy (kJ mol^{-1})	Exothermicity (Q/J mol^{-1})
Initiation	$P \rightarrow A$	$A_i = 1 \times 10^{-6}$	$E_i = 0$	0
Propagation	$A \rightarrow B$	$A_p = 1 \times 10^{6}$	$E_p = 0$	0
Termination 1	$A \rightarrow C$	$A_{t1} = 1 \times 10^{11}$	$E_{t1} = 75$	0
Branching	$B \rightarrow 2A$	$A_b = 8 \times 10^{3}$	$E_b = 45$	1×10^{5}
Termination 2	$B \rightarrow C$	$A_{t2} = 0.60$	$E_{t2} = 0$	0

energy conservation equation is included here in addition, yielding a three-variable model, represented by the concentrations of A and B and the reactant temperature T. The relevant, fully dimensional conservation equations are as follows, where the elementary rate constants are represented by k and the concentrations of the respective species are denoted by lowercase letters.

$$\frac{\partial a}{\partial t} = k_i p_o e^{(-k_1 t)} - k_{t1}(T)a - k_p a + 2k_b(T)b + D_A \nabla^2 a \quad (1)$$

$$\frac{\partial b}{\partial t} = k_p a - k_b(T)b - k_{t2} b + D_B \nabla^2 b \quad (2)$$

$$\frac{c\partial T}{\partial t} = \frac{Qk_b(T)b}{C_v \sigma} - \frac{1(T - T_a)}{t_N} + D_T \nabla^2 T \quad (3)$$

The Lewis number, Le, is defined as D_T/D_A. Both Newtonian and diffusive thermal heat transport terms are included in the energy conservation equation. These were flagged to permit adoption of either spatially uniform or diffusive heat transport conditions in the numerical procedure described in the next section. An additional option in the diffusive flux-driven calculations was to choose boundary conditions that reflected either total loss or no loss of the autocatalytic intermediate at the surface. The boundary conditions were, in each case,

$$\frac{\partial a}{\partial x} = 0 \text{ and } \frac{\partial T}{\partial x} = 0 \text{ at } x = 0 \quad (4)$$

$$\frac{\partial T}{\partial x} = 0 \text{ at } x = r,$$

for spatially uniform conditions (5)

$$(T - T_a) = 0 \text{ and (optionally) } b = 0 \text{ at } x = r,$$

for purely conductive conditions (6)

Heat capacity and reactant density were taken to be 105 J mol^{-1} K^{-1} and 8.2×10^{-6} mol cm^{-3}, respectively, and the (constant) volumetric heat capacity was 8.6×10^{-4} J m^{-3} K^{-1}. The chosen density corresponds to an initial reactant pressure of 40 kPa at 600 K, which is typical of the experimental conditions [9]. The numerical results are not strongly sensitive to the heat capacity and not at all sensitive to the reactant density because it is not involved in subsequent steps. The requirement for oxygen may be regarded to be subsumed in the (pseudo) first-order rate parameters. The simulations represent experiments in a 500 cm^3 spherical vessel.

Numerical Methods

Equations 1–3, subject to boundary conditions 4–6, were cast in non-dimensional form, representing the classical one-dimensional shapes (infinite slab, infinite cylinder, or sphere), and integrated using the numerical algorithm group (NAG) routine D03PSF [12]. This routine is set up for the integration of a system of nonlinear convection–diffusion equations in one dimension, using the method of lines to reduce the partial differential equations to ordinary differential equations (ODEs). The ODE system is then solved by a backward difference (BDF) method [13]. The BDF algorithm makes use of formulae, the order of which are varied automatically up to order 5. The scheme is an implicit, variable step-size method, the time step and order being selected automatically to satisfy a user-specified tolerance. This allows temperature spikes, which may develop on very short time scales, to be accurately modeled while not restricting the time step in other phases of the simulation. A modified Newton iteration scheme is used to solve the system of nonlinear equations at each time step.

The problem was discretized using a finite volume approach [12]. The source terms were calculated at each node, and the diffusive terms were evaluated at each nodal midpoint using values derived from the nodes at either side [14]. These values were calculated by assuming that the solution varied within a cell and employed standard upwind techniques combined with a slope limiter [15]. In the present application, the domain was meshed uniformly with 126 points. Neumann conditions were specified at the symmetry boundary, and a mixture of Neumann

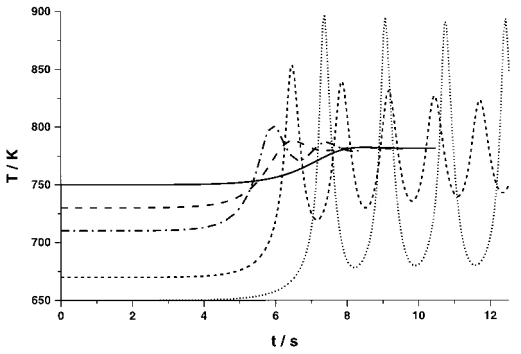

FIG. 1. Temperature-time profiles from the integration of equations 1–3 under spatially uniform conditions at t_N = 0.2 s. The initial and boundary temperatures are respectively 650–750 K in 20 K increments. This spans the transition from sustained oscillations through damped oscillatory reaction to stable stationary state reaction. The sustained oscillations set in at T_a = 590 K.

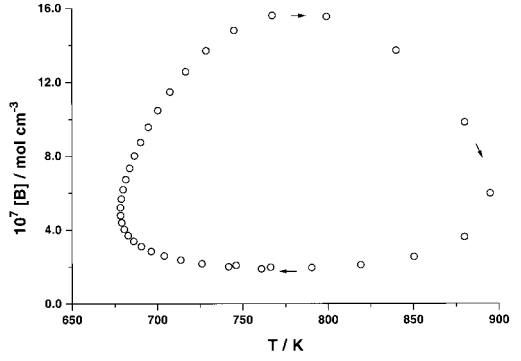

FIG. 2. A phase plane map representing the relationship between the concentration of intermediate B and reactant temperature over the time interval 7.8–9.5 s at T_a = 650 K (see Fig. 1). The rise and fall of [B] is predicted to precede that of T, as marked by the arrows.

and Dirichlet conditions were specified at the outer boundary, as noted above.

The code, D03PSF, provides accuracy up to order 5 for a single time step. For a number of time steps, the local error tolerances were investigated, and values were chosen that did not compromise the solution. For spatial accuracy, the solutions from different numbers of mesh points were compared. The chosen number reflected a satisfactory compromise between computational speed and solution accuracy.

Results and Discussion

Spatially Uniform Conditions

A Newtonian cooling time (t_N) of 0.2 s was assigned to the system, which is a reasonable representation for a well-stirred closed system [16]. The results of the simulations for temperature versus time over a vessel temperature range 650–750 K are shown in Fig. 1. The onset of sustained oscillations occurs at 590 K (not shown), which is set by the magnitude of A_{f2}, but there is a transition to a damped oscillatory state at about T_a = 660 K (Fig. 1). The damped oscillations converge to a fixed stationary state temperature (T = 782 K), corresponding to that attained in the stable, non-oscillatory high-temperature state, at T_a > 740 K. The fixed value for the final reactant temperature is consistent with the response to an ntc of reaction rate in hydrocarbon combustion, as observed experimentally in the combustion of alkanes following rapid compression [17] and in propane combustion in a high-pressure flow reactor [18].

Phase relationships can be distinguished when stable oscillations occur, as shown in the two-dimensional phase plane for the relationship between the concentration of B and the temperature T during oscillations at 650 K (Fig. 2). The maximum in the concentration of B precedes the maximum of T in each cycle. The concentrations of the intermediates A and B rise and fall in phase, and so are not shown.

Spatially Non-uniform Conditions

Spatially non-uniform behavior was generated as a result of diffusive fluxes for mass and energy, taking $D_A = D_B = 3\ cm^2\ s^{-1}$ and $Le = 1$, with no loss of B following diffusion to the surface. The diffusion coefficient would not normally be expected to exceed this value [5]. Sustained oscillations were not detected at any temperature under these conditions, the only manifestation being that of highly damped oscillations to a stationary state (Fig. 3). The temperature records in Fig. 3 relate to behavior at the center of the vessel. Further study of the domain of D_A showed that sustained oscillations could be established under the effect of diffusive fluxes, for example, at the hypothetical case at $D_A > 15\ cm^2\ s^{-1}$ ($Le = 1$) when T_a = 590 K, but rising to $D_A > 30\ cm^2\ s^{-1}$ at T_a = 650 K (see later). An experimental pressure record from the microgravity experiments is also shown in Fig. 3. There is a relatively slow entry of reactants, during which time the reaction develops to a damped oscillatory state, exemplified by the initial overshoot in pressure, followed by a limited number of smaller amplitude oscillations [9].

The spatial variations associated with the development of reaction were also investigated with respect to temperature and intermediate product concentrations over a range of conditions. These are illustrated in Figs. 4 and 5 at the threshold of the sustained oscillatory mode, for which T_a = 590 K at $Le = 1$. The response of the three variables over the time interval 12.52–13.41 s, corresponding to the initial temperature excursion, is shown in Fig. 4. The temperature develops earliest at the center of the

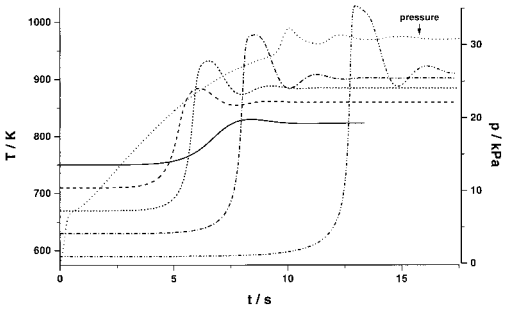

FIG. 3. Temperature-time profiles from the integration of equations 1–3 in one dimension (spherical symmetry) under diffusive heat and mass fluxes, $D_A = D_B = D_T = 3\ cm^2\ s^{-1}$. The initial and boundary temperatures are, respectively, 590–750 K in 40 K increments. This spans the full range from the onset of damped oscillatory reaction to stable stationary state reaction. No sustained oscillations were predicted at these conditions. An experimental pressure record from the microgravity experiments is also shown. This was obtained from the mixture 0.25 C_4H_{10} + 0.25 O_2 + 0.5 Ar entering a reaction vessel at 583 K to an initial pressure of 29 kPa.

sphere, but the successive temperature profiles (12.85–13.27 s) convey a sense of the outward development of a combustion front (Fig. 4a). This is not a self-sustained combustion wave insofar that it does not propagate fully to the surface.

Both *A* and *B* exhibit maxima in their concentrations which are displaced outward throughout the time period of the thermal records in Fig. 4a (Fig. 4b and c). The maxima of *A* and *B* are not coincident in time and space, however. The progress of the peak concentration of *A* toward the edge of the reaction vessel (Fig. 4b) is reminiscent of the symmetrical expansion of the chemiluminescent region observed experimentally [9]. The intermediates are almost entirely consumed at the center of the system in the later stages. Whereas *B* is able to accumulate at the surface to yield its highest concentrations there in the late stages of the thermal cycle, a marked gradient in the concentration of *A* is predicted at the surface. The minor oscillations in Fig. 4b are a numerical artifact.

The evolution during the time period from 13.69 s to 14.81 s is depicted in Fig. 5a–c, and this corresponds to the interval during which the center temperature relaxes from its maximum at about 1000 K to around 890 K (see Fig. 3). Just at the end of this time period, there is a thermal response to chemical activity at about 2.5 cm along the radius (Fig. 5a). This distorts the thermal profile to a virtually flat central region ($t = 15.09$ s) which, in the subsequent stage of reaction, evolves to a slight dip in temperature toward the vessel center ($t = 15.51$ s). There is no substantial qualitative change throughout the

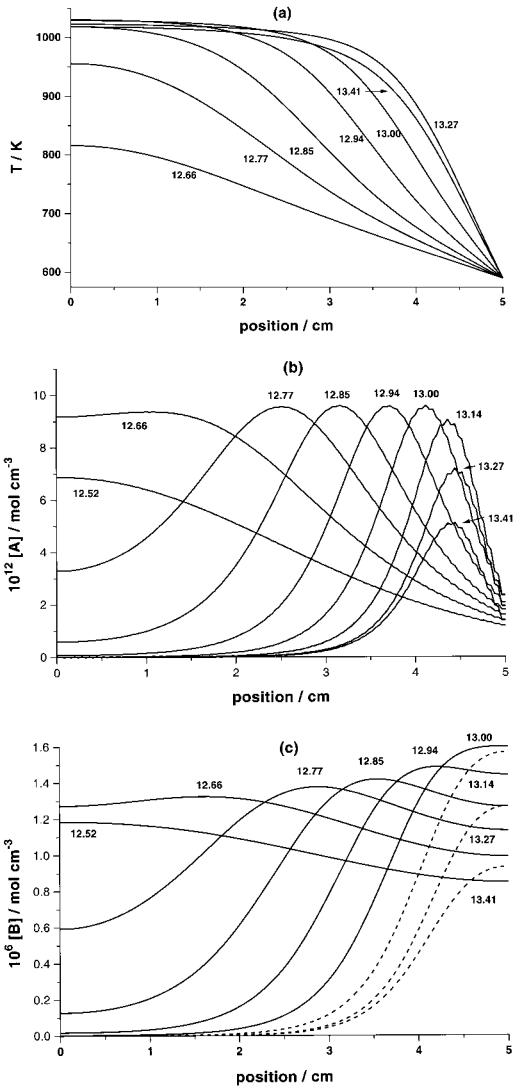

FIG. 4. The predicted evolution of the spatial distributions of (a) temperature *T*, (b) intermediate species *A*, and (c) intermediate species *B* across a radius of the spherical mass at selected times during reaction at $T_a = 590$ K. The respective times are marked, and they correspond to the period for the development of the initial temperature peak. The minor fluctuations in the profiles for *A* arise from the choice of output frequency of data points and the mesh. The broken lines signify profiles for which there has been a change of direction in the temporal evolution.

respective spatial concentration profiles of *A* or *B* (Fig. 5b and c), and the growth in chemical activity is confined to the outer regions of the reactor. Once the initial thermal gradient has developed, mass and thermal diffusion seem not to be sufficient to affect the behavior in other regions.

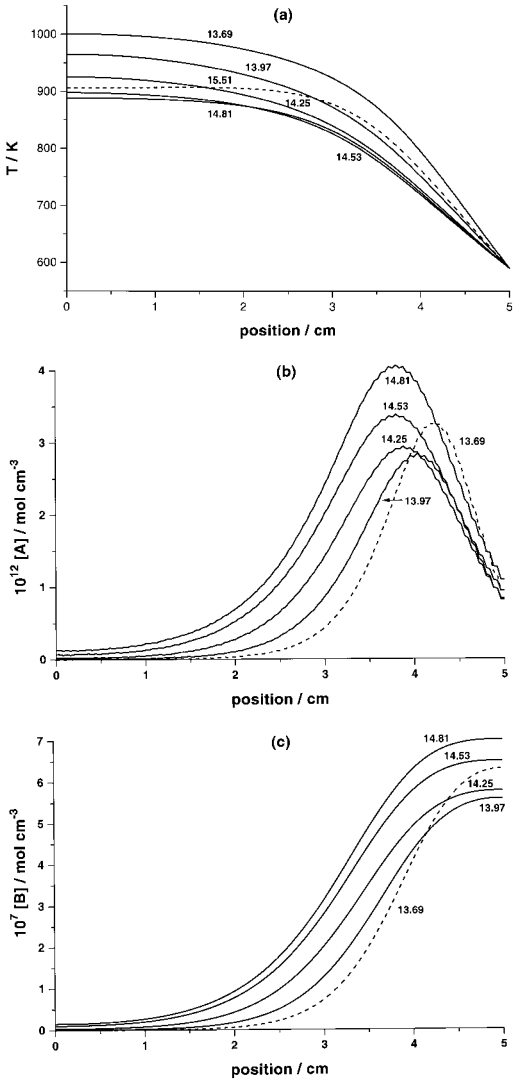

FIG. 5. The predicted evolution of the spatial distributions of (a) temperature T, (b) intermediate species A, and (c) intermediate species B across a radius of the spherical mass at selected times during reaction at $T_a = 590$ K. The respective times are marked. They correspond to the period during which there is a relaxation of the first temperature peak and development of the second one. A slightly later temperature profile is also shown in which the temperature at 2.0 cm exceeds that at the center. The broken lines signify profiles for which there has been a change of direction in the temporal evolution.

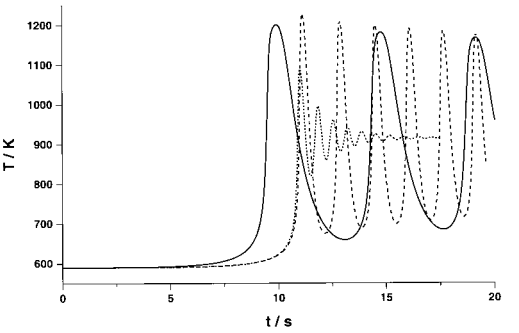

FIG. 6. Temperature–time profiles from the integration of equations 1–3 in one dimension (spherical symmetry) under the respective diffusive heat and mass fluxes. Full line, $D_A = D_B = 16$ cm^2 s^{-1}, $D_T = 3$ cm^2 s^{-1} ($Le = 0.1875$); broken line, $D_A = D_B = D_T = 16$ cm^2 s^{-1} ($Le = 1$); dotted line, $D_A = D_B = 3$ cm^2 s^{-1}, $D_T = 16$ cm^2 s^{-1} ($Le = 5.33$). The initial and boundary temperatures are 590 K. These results support the interpretation that the mass diffusion is the dominant term in determining whether or not sustained cool flame oscillations can occur under the influence of diffusive fluxes.

To what extent then does the limitation on mass or thermal diffusion cause the failure of sustained oscillations? The enhancement of both diffusive processes provokes sustained oscillations, as shown in the thermal record at $D_T = 16$ cm^2 s^{-1}, $Le = 1$ (Fig. 6). There is the same qualitative effect when $D_T = 3$ cm^2 s^{-1} and $D_A = 16$ cm^2 s^{-1}, at $Le = 0.1875$ (Fig. 6). How the rate of heat loss by the enhancement of D_T affects the oscillatory frequency can also be seen in Fig. 6. Reversing the diffusivities so that $D_T = 16$ cm^2 s^{-1} ($Le = 5.33$) allows only highly damped oscillations to occur throughout the temperature range. Spatial temperature and concentration changes for B associated with the time period 13.70–15.30 s at $Le = 0.1875$ are shown in Fig. 7. Clearly, in these circumstances the diffusion of B is sufficiently high to reduce the intermediate species concentration at the periphery of the reaction vessel, which has a consequence on the reaction rate throughout the system.

Conclusions

When a perfectly mixed state exists, both sustained and damped oscillatory modes are predicted to occur using a thermokinetic model to represent hydrocarbon oxidation in the cool flame region. By contrast, heat and mass transport under normal, diffusive conditions are not sufficiently high to promote sustained oscillations. The diffusive fluxes have to be raised to rather higher values for sustained oscillations to be induced. Nevertheless, damped oscillatory reaction states can exist at normal diffusivities,

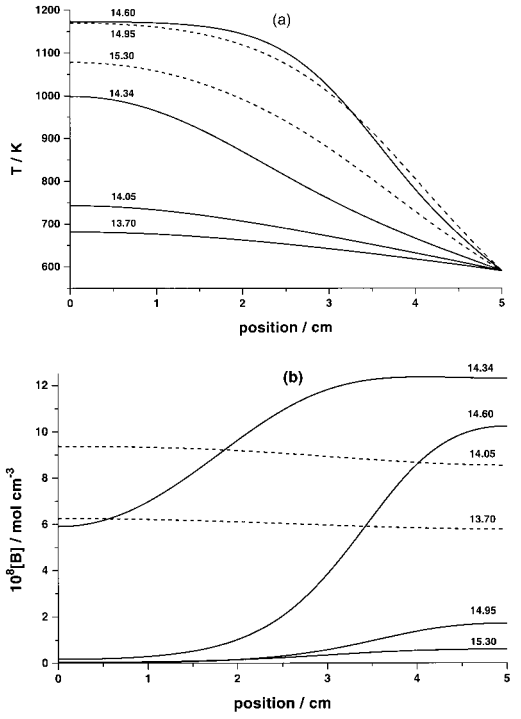

FIG. 7. The predicted evolution of the spatial distributions of (a) temperature T and (b) intermediate species B across a radius of the spherical mass at selected times during reaction at $T_a = 590$ K for the conditions $D_A = D_B = 16\,cm^2\,s^{-1}$, $D_T = 3\,cm^2\,s^{-1}$ ($Le = 0.0625$). The respective times are marked. They correspond to the period in which the second cool flame develops and subsides. The broken lines signify profiles for which there has been a change of direction in the temporal evolution.

which are a manifestation of cool flame activity and would appear visually as a single cool flame.

The failure to generate sustained oscillations is attributed to the accumulation of reactive intermediates in the outer reaches of the reacting mass, where the temperature is lowest (Figs. 4 and 5), so that the chemical activity is then sustained in these localized regions and cooling in the center cannot then occur. The dispersion of the intermediates by enhanced mass diffusion causes a major qualitative change, such that sustained oscillations are then possible.

An alternative route to reduction of the intermediate concentration in the periphery of the vessel would be to promote surface termination. However, if the boundary conditions are transformed to permit full destruction of B at the surface, as in equation 6, this so diminishes the reactivity that strong exothermic reaction becomes possible in reasonable timescales only at $T_a > 650$ K, where highly damped oscillations are inevitable. This is consistent with the experimentally observed suppression of cool flames when efficient chain terminating surfaces are used [19]. There was also no indication of a propagating front when these boundary conditions were applied.

It is not intended to imply that the limiting diffusion coefficients or Lewis numbers given here could be accessible experimentally or, indeed, that the same limits would necessarily prevail if a comprehensive kinetic scheme to represent normal butane oxidation were investigated numerically in a one-dimensional model. However, we believe that these are the first indications of how the generation of multiple cool flames of hydrocarbons are affected by heat and mass transport as a result of diffusion. Confirmation has been gained in subsequent experiments by Pearlman et al. when helium has been used as a diluent.

REFERENCES

1. Griffiths, J. F., Gray, B. F., and Gray, P., *Proc. Combust. Inst.* 13:239–248 (1971).
2. Griffiths, J. F., and Mohamed, C., in *Low Temperature Oxidation of Hydrocarbons, Comprehensive Chemical Kinetics, Vol. 35,* (M. J. Pilling, ed.), Elsevier, Amsterdam, pp. 545–660.
3. Curran, H. J., Pitz, W. J., Westbrook, C. K., Callahan, C. V., and Dryer, F. L., *Proc. Combust. Inst.* 27:379–387 (1998).
4. Semenov, N. N., *Chemical Kinetics and Chain Reactions,* Clarendon Press, Oxford, U.K., 1935.
5. Frank-Kamenetskii, D. A., *Diffusion and Heat Transfer in Chemical Kinetics,* Plenum, New York, 1969.
6. Ashmore, P. G., Tyler, B. J., and Wesley, T. A. B., *Proc. Combust. Inst.* 11:1133–1140 (1967).
7. Fine, D. H., Gray, P., and Mackinven, R., *Proc. R. Soc. Lond. A* 316:223–260 (1970).
8. Amemiya, T., Kadar, S., Kettunen, S., and Showalter, K., *Phys. Rev. Lett.* 77:3244–7 (1996).
9. Pearlman, H., *Combust. Flame* 121:390–393 (2000).
10. Yang, C. H., and Gray, B. F., *J. Phys. Chem.* 73:3395–3406 (1969).
11. Gray, P., and Scott, S. K., *Chemical Oscillations and Instabilities,* Clarendon Press, Oxford, U.K., 1990.
12. Pennington, S. V., and Berzins, M., *ACM Trans. Math. Software* 20:63–99 (1994).
13. Berzins, M., *Appl. Numer. Anal.* 2:109–118 (1986).
14. Skeel, R. D., and Berzins, M., *SIAM J. Sci. Stat. Comp.* 11:1–32 (1990).
15. Van Leer, B., *J. Comp. Phys.* 14:361–370 (1974).
16. Griffiths, J. F., *Annu. Rev. Phys. Chem.* 36:77–104 (1985).
17. Griffiths, J. F., Halford-Maw, P., and Rose, D. J., *Combust. Flame* 95:291–304 (1993).
18. Koert, D. N., Miller, D. L., and Cernansky, N. P., *Combust. Flame* 96:34–49 (1994).
19. Chernesky, M., and Bardwell, J., *Can. J. Chem.* 38:482–492 (1960).